Optimal Experiment Design for Calibrating an Airpath Model of a Diesel Engine

Ioanna Stamati[1], Dries Telen[1], Filip Logist[1], Eva Van Derlinden[1], Markus Hirsch[2], Thomas Passenbrunner[2], Jan Van Impe[1*]

[1] BioTeC & OPTEC, Chemical Engineering Department, Katholieke Universiteit Leuven, W. de Croylaan 46, 3001 Leuven, Belgium; **jan.vanimpe@cit.kuleuven.be*

[2] Institute for Design and Control of Mechatronical Systems, Johannes Kepler University, Linz, Austria

Abstract. Mathematical models become more and more indispensable tools for engine manu- facturers. As nonlinear dynamic models based on first-principles are preferred by practitioners, model calibration or parameter estimation is often a time consuming task. The use of optimally designed dynamic inputs can reduce the experimental burden and increase the accuracy of the estimated parameters. The current paper presents the calibration and validation of a Diesel engine airpath model. Optimal inputs have been designed based on random phase multisine inputs. These multisines can be adapted to excite exclusively a specific frequency band of interest. Moreover, they allow (i) to concentrate the input around an operating point, and (ii) to include fast variations in the input profile without introducing a large number of discretization parameters. The resulting model has been found to provide an acceptable predictive power in both identification and validation.

Introduction

Mathematical models and simulations are more and more exploited for the analysis, design, operation and optimiza- tion of engines (Stewart et al., 2011). However, the accurate modelling of engine processes is often a non-trivial task. There are several reasons or this. First, many of these processes are intrinsically *dynamic* in nature, i.e., properties and variables vary over time, giving rise to dynamic models. As often fast and slowly varying variables are present, different time scales have to be accounted for. Moreover, *mechanistic* models, which start from the physical principles and conservation laws underlying the process, are preferred in practice because of their generic prediction capabilities.

However, the underlying mechanisms often require highly nonlinear model descriptions. Mathematically, this kind of description results in non-linear ordinary differential equation (ODE) models. In addition, before the models can be employed in practice for the above mentioned purposes, *model calibration* or *parameter estimation (PE)* is required, i.e., estimating the unknown parameters based on experimental data. As experiments can be time consuming and expensive, Optimal Experiment Design (OED) techniques are attractive to reduce the experimental burden (Walter and Pronzato, 1997). Here, optimal inputs are designed such that outputs are as informative as possible with respect to the target parameter(s).

In the current paper dynamic parameters of an airpath model for a Diesel engine have to be estimated. The airpath model used is similar to the one described in Puchner et al. (2009) and the dynamic parameters have to be estimated based on measurement from an engine test bench.

In the current case, two specific requirements are present. Fast variations in the designed inputs have to be combined with long time horizons and (too) large deviations from specified setpoints have to be avoided. This combination prohibits the use of polynomial discretizations which are typically employed (Franceschini and Macchietto, 2008). Hence, procedures based on multisine input representations have been developed and successfully been applied.

The paper is organized as follows. Section 1 details the Engine test bench and the airpath model under study. In Section 2 the Optimal Experiment Design strategy is outlined whereas in Section 3 the overall approach is pointed out. Section 4 discusses the obtained results. Finally, the conclusions are summarized in Section 5.

SNE Simulation Notes Europe – Print ISSN 2305-9974 | Online ISSN 2306-0271
SNE 22(3-4), 2012, 121-128 | doi: 10.11128/sne.22.tn.10139

1 Engine Test Bench and Airpath Model

1.1 Engine Test Bench

The device under investigation is a 2 liter EU5 common rail Diesel engine with external exhaust gas recirculation and a variable geometry turbine turbocharger. This new engine replaces the BMW M47T-OL Diesel engine used in Alberer (2009); Ferreau et al. (2007); Puchner et al. (2009)).

Figure 1 presents a schematic view of the engine's air path. It consists of the intake and exhaust manifold, a path for the Engine Gas Recirculation (EGR) (i.e., EGR-valve and EGR-cooler), the Variable Geometry Turbocharger (VGT) with the intercooler and the cylinder block with the swirl flaps. Five variables can be manipulated, i.e., position of EGR and VGT valve, injected fuel mass, engine speed and swirl state, while measured variables involve the intake pressure (MAP), fresh air flow (MAF), the oxygen concentration in the exhaust, the oxygen concentration in the intake manifold and the crankshaft torque.

1.2 Airpath model

The model is characterized by the combination of physical equations with static maps. The maps mainly capture the static behavior of the engine, while physical equations (e.g., the ideal gas equation and equations for conservation of mass and energy) account for the dynamic behavior. These maps are derived based on steady-state test-bench measurements and are used for polynomial interpolation- extrapolation between process variables (Alberer, 2009).

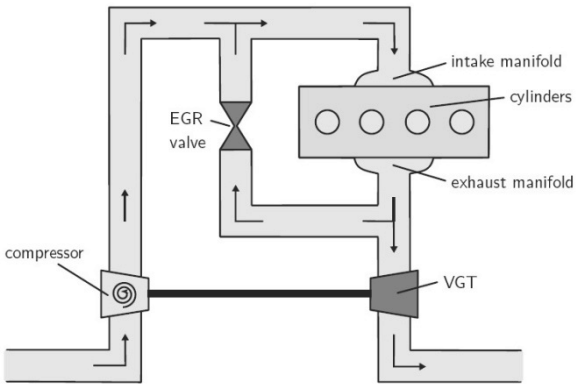

Figure 1. Schematic diagram of the Diesel airpath System (Ferreau et al., 2007).

The airpath model is provided as a `Simulink` file which can be run from `Matlab`. It has as inputs **u** the five manip- ulated variables, i.e., EGR valve position X_{egr}, the VGT activation signal X_{vgt}, the engine speed n, the injected fuel mass W_{f} and the swirl valve position. The outputs are the five mentioned measured variables, i.e., the intake pressure (MAP), fresh air flow (MAF), the oxygen concentration in the exhaust, the oxygen concentration in the intake manifold and the crankshaft torque. However, for practical reasons not all inputs and outputs have been incorporated in the Optimal Experiment Design. For instance, the swirl valve which can only be either entirely open or closed, has been assumed to be constantly open. In addition, only the in practice more easily measurable intake manifold pressure and flow have been considered to be available.

The model contains five parameters describing the dynamic behavior, which have to be estimated (i.e., *Parameter Estimation* task (PE)). These parameters are the volume of the intake and exhaust manifold V_{i}

and V_{x}, the turbocharger efficiency η_{n} and the time constants of the turbocharger and the exhaust gas recirculation cooler τ_{vgt} and τ_{egr}. Hence, the four model inputs X_{egr}, X_{vgt}, n and W_{f} have to be designed in order to yield as informative outputs for MAF and MAP as possible (i.e., *Optimal Experiment Design* task (OED)). These two outputs mentioned above will be used for model calibration.

2 Optimal Experiment Design for Nonlinear Dynamic Systems

2.1 Optimal Control Problem

Optimal Experiment Design for nonlinear dynamic systems described by Ordinary Differential Equations gives rise to a particular class of optimal control problems.

$$\min_{\mathbf{u}} J \tag{1}$$

subject to

$$\frac{d\mathbf{x}}{dt} = \mathbf{f}(\mathbf{x}(t), \mathbf{u}(t), \mathbf{p}, t) \quad t \in [0, t_f] \tag{2}$$

$$\mathbf{0} = \mathbf{b}_c(\mathbf{x}(0), \mathbf{p}) \tag{3}$$

$$\mathbf{0} \geq \mathbf{c}_p(\mathbf{x}(t), \mathbf{u}(t), \mathbf{p}, t) \tag{4}$$

Here, **x** are the state variables, **u** the time-varying control inputs and **p** the model parameters.

The vector **f** represents the dynamic system equations (on the interval $t \in [0, t_f]$) with initial conditions given by the vector $\mathbf{b}_c$ .The vector $\mathbf{c}_p$ indicates path inequality constraints on states and controls. **y** are the measured outputs, which are typically a subset of the state variables **x**.

2.2 Objective Function

In OED, the objective function J is typically a scalar function Φ of the Fisher information matrix

$$\mathbf{F}(\mathbf{p}) = \sum_{i=1}^{n_t} \left(\frac{\partial \mathbf{y}(\mathbf{p}, t_i)}{\partial \mathbf{p}}\right)^T \mathbf{Q} \left(\frac{\partial \mathbf{y}(\mathbf{p}, t_i)}{\partial \mathbf{p}}\right) \qquad (5)$$

with n_t the number of measurement times t_i. **F** combines information on (i) the error on the output measurements (**Q** is typically defined as the inverse of the measurement error variance matrix), and (ii) the sensitivities of the model output (**y**(**p**, t_i)) to small variations in the model parameters **p** (expressed in the sensitivity matrix $\frac{\partial \mathbf{y}(\mathbf{p},t_i)}{\partial \mathbf{p}}$). To this end several scalar criteria have been described in literature, e.g.:

A-criterion **min[trace($\mathbf{F}^{-1}$)].** A-optimal designs minimize the arithmetic mean of the parameter estimation errors. This corresponds to the minimization of the sum of the squared axes of the asymptotic joint confidence region, i.e, minimizing the frame enclosing this confidence region.

D-criterion **max[det(F)]**. The D-criterion minimizes the geometric mean of the parameter estimation errors. D-optimal design aims at the minimization of the parameter estimation variance-covariance, i.e., minimization of the joint confidence region on **p** via the maximization of the determinant of **F**.

E-criterion **max[λ_{min} (F)]**. E-optimality focuses on the minimization of the largest parameter error (i.e., maximization of the smallest eigenvalue), and as such, neglects uncertainty on the remaining parameters. This corresponds to minimizing the longest axis of the joint confidence region

2.3 Input Discretization and Degrees of Freedom

Nowadays optimal control problems are most often solved by direct approaches which convert the infinite dimen- sional optimal control problem into a finite dimensional nonlinear program by discretizing the control resulting in a finite number of degrees to be optimized.

Typically, piecewise polynomial discretizations are used (Biegler, 2007; Diehl et al., 2002). As in mechatronic systems fast variations have to be combined with long time horizons, piecewise constant control discretizations yield a too high number of control parameters to be optimized. To tackle this issue, in the current paper three strategies based on *random phase multisines* are proposed (Pintelon and Schoukens, 2001)

$$u(t) = u_0 + \sum_{k=1}^{F} \left(A_k \cos(2\pi f_k t + \varphi_k)\right) \qquad (6)$$

where u_0 is the operating point to be chosen, f_k are the frequencies and A_k are the cosine amplitudes, F is the number of frequency domain data samples and φ_k is a random phase. This kind of signals has the advantage that (i) energy can be concentrated in the dominant frequency ranges of the system and that (ii) they are most interesting when designed inputs are preferred around pre-specified operating points .

2.4 Optimization Strategies

In general, multisines exhibit three classes of degrees of freedom that can be optimized. The *root mean square* value (RMS) of the signal belongs to the first class. For a signal $u(t)$ with n_t points, the RMS is defined as:

$$\text{RMS} = \sqrt{\frac{1}{n}\sum_{n} u^2(t_i)} \qquad (7)$$

The RMS value is calculated based on the signal after subtraction of the operating point. The frequency bands compose the second class of degrees of freedom, while the last class of degrees of freedom involves the amplitudes A_k of the cosines. Depending on the selected class of degrees of freedom, different strategies are obtained. For a schematic representation see Figure 2.

In the first strategy (S1 or *RMS optimized*) only the RMS value of the multisine is optimized. This means that both the frequency band of the signal as well as the amplitudes of the different frequency contributions remain at pre- specified values.

Optimizing the frequency bands is the second strategy (S2 or *frequency optimized*). The advantage is that a frequency band can be selected that excites the outputs the most. Consequently, more information can be obtained by exciting a specific frequency band. During this optimization the RMS value is kept constant and the amplitude remains the same in the whole band.

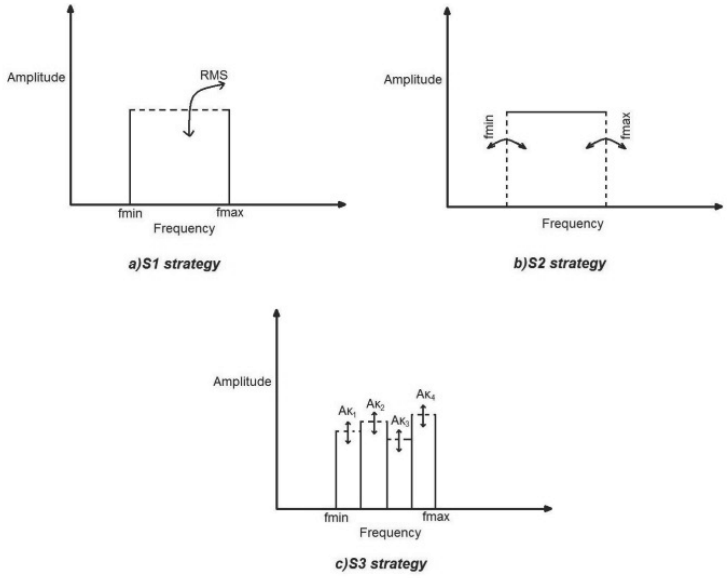

Figure 2. Schematic diagram of the different input structures.

The third strategy (S3 or *amplitude optimized*) requires to vary the amplitudes of the different frequencies. For every frequency band, the band is divided in four different parts which are allowed to have a different amplitude.

Four different subbands for each signal are chosen in order not to increase the number of decision variables too much and by doing so to limit the increase in the computation time. The amplitudes are optimized together with the RMS value.

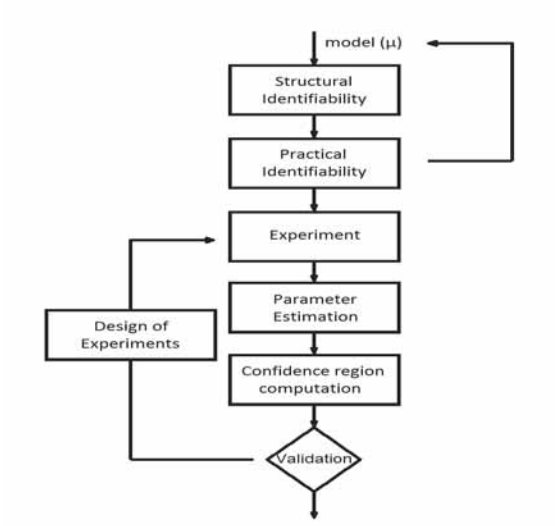

Figure3. Schematic diagram of the modeling cycle.

3 Procedure

This section outlines the global approach that has been used. Under the assumption that a correct model struc-ture is selected for the underlying dynamic process, the model parameters need to be estimated.

This can be done according to the general modeling procedure or so-called *modeling cycle* (Balsa-Canto et al., 2010; Franceschini and Macchietto, 2008; Ljung, 1999; Walter and Pronzato, 1997).

The preliminary step in the *modeling cycle* involves a verification of the model's structural and practical identifiability. A sensitivity analysis of the outputs with respect to the inputs will in this respect often reveal quite some information. If this step succeeds, then a sequential approach follows for choosing the appropriate parameters as can be seen in Figure 3. This sequential part includes the loop: *Experiment*, *Parameter Estimation*, *Confidence Interval Computation* and *Design of Experiments* according to the results of the Confidence Interval. This sequential procedure will be applied in the current study.

3.1 Sensitivity analysis

An important background step for experiment design is sensitivity analysis. An analysis of the sensitivity functions can provide insight in (i) which parameters have the largest influence and, hence, have to be estimated preferably and (ii) which experimental conditions enclose the most information for the accurate estimation of specific parameters.

3.2 Design of Experiments

The Design of Experiments provides new inputs for the Parameter Estimation. As Design of Experiments involves an optimization problem, first the criterion has to be selected among the available ones (Section 2.2). As a next step the type of input signal as well as the parameters characterizing the signal have to be selected. In the current work the E-criterion: $\max[\lambda_{min}(\mathbf{F})]$ is selected with input structures according to the above three strategies.

3.3 Parameter Estimation

Given a designed input, an experiment can be performed and a parameter estimate can be obtained.

Parameter Estimation involves the selection of parameter values such that the model predictions $\mathbf{y}(\mathbf{p}, t_i)$ fit the measurements $\mathbf{y}_{exp}(t_i)$ as accurately as possible despite the presence of measurement errors. The most common assumption about the probability distribution of the measurement errors is that they are additive, independent and identically distributed according to a Gaussian distribution. These assumptions typically lead to a *sum of squares* objective (Walter and Pronzato, 1997):

$$\boldsymbol{J}(\mathbf{p}) = \sum_{i=1}^{n_t} \left(\mathbf{y}(\mathbf{p}, t_i) - \mathbf{y}_{exp}(t_i)\right)^T \mathbf{Q} \left(\mathbf{y}(\mathbf{p}, t_i) - \mathbf{y}_{exp}(t_i)\right)^T \quad (8)$$

with n_p the number of parameters and n_t the number of measurements. The *weighting matrix* **Q** is typically selected as the inverse of the measurement error variance- covariance matrix.

3.4 Confidence Intervals Computation

The quality of a parameter estimate, or vice versa, its uncertainty, is quantified by its variance or standard deviation, which is a measure for the spread of the parameter distribution. Parameter variances can be extracted from the parameter variance-covariance matrix **P**:

$$\mathbf{P} = E[(\mathbf{p}^* - \hat{\mathbf{p}})\,(\mathbf{p}^* - \hat{\mathbf{p}})^T] \quad (9)$$

with $\mathbf{p}^*$ and $\mathbf{p}\hat{}$ the true and estimated parameter vector, respectively. The variance-covariance matrix **P** can be approximated by the inverse of the *Fisher information matrix* (for more details see Walter and Pronzato (1997)). The variances s_i on the main diagonal of **P** can be used to determine the (1-α)100% confidence interval for each parameter estimate

$$\left[\hat{p}_i - t_{\left(1-\frac{\alpha}{2}, n_t - n_p\right)}\sqrt{s_i^2}, \hat{p}_i + t_{\left(1-\frac{\alpha}{2}, n_t - n_p\right)}\sqrt{s_i^2}\right] \quad (10)$$

with t the Student-t value for $n_t - n_p$ degrees of freedom, (1-α) the confidence level, n_t the number of experimental data points and n_p the number of estimated parameters.

3.5 Implementation

The airpath model is provided as a `Simulink` file that can be called from `Matlab`. Due to model specifications the sensitivity functions have to be approximated using a finite difference approach in the current work.

For the PE the `lsqnonlin Matlab` function is used. It is a gradient based method but the gradients are computed using first-order finite difference perturbations. For the Confidence Intervals the Student-t value from Matlab is used, and the variance-covariance matrix is calculated with outputs of the PE procedure. Finally for the OED the fmincon Matlab function is used for the optimization whereas the sensitivities are calculated with finite differences as well.

4 Results

In this section the results for the airpath model will be presented. First, it has been seen from the sensitivity analysis that all parameters have an influence on at least one of the outputs. Hence, this strengthens the believe that all parameters can be estimated (when appropriate inputs are applied).

However, in view of conciseness, plots of the sensitivities have been omitted. Second, inputs have been optimized based on each of the three strategies. Every strategy was applied on four different operating points (O.P.) as defined in Table 1. Also a comparison to white noise has been made. Third, the designed inputs have applied to the testbench and parameters have been estimated. Finally, a validation of the calibrated model has been performed.

O.P.	X_{egr} [%]	X_{vgt} [%]	n[*rpm*]	W_{f} [*mg/cyc*]
1.	40	85	1500	15
2.	40	75	2000	15
3.	55	80	1800	7
4.	20	70	2200	25

Table 1. Operating points.

4.1 Optimization Strategy Comparison

During the entire procedure the sampling time is 0.01 s and the duration of the cycle is 20 s. The frequency resolution is 0.05 Hz. Due to the practical implementation issues the upper bound on the frequency bands are constrained to $X_{egr} \leq 10$ Hz, $X_{vgt} \leq 5$ Hz,$n \leq 2$ Hz and $W_f \leq 4$ Hz.

The random phases are chosen to be random values in the interval [0, 2π). The given measurement variance for MAP is $\sigma^2_{\mathrm{MAP}}=100^2$ and for MAF is $\sigma^2_{\mathrm{MAF}}=10^2$.

S1 Strategy. In a first optimization approach only the RMS value of the four multisines added to the operating points is optimized. This means that both the frequency band of the four signals as well as the amplitudes of the different frequency contributions remained the same in the entire frequency range.

The resulting minimal eigenvalues are summarized in Table 2. Operating points 2 and 4 are of higher information.

		RMS value			
O.P.	λmin	X_{egr}	X_{vgt}	n	W_{f}
1.	3.79*e*03	12.75	4.78	184.42	4.04
2.	2.92*e*06	12.24	0.03	300.00	2.52
3.	2.46*e*03	12.16	7.88	259.66	1.99
4.	1.99*e*07	5.10	8.00	194.34	1.50

Table 2. RMS optimization results.

S2 Strategy. The effect of optimizing the frequency bands is exploited in the second strategy. The idea is that the system can be excited in a certain band. As a result, more information can be obtained by exciting a specific frequency band.

The RMS value and the amplitudes are kept constant in this approach. The RMS values are tuned at the values obtained in the previous strategy. In Table 3 there is an overview of the obtained frequencies as well as the used RMS values. For operating points 1 and 3 a higher λ_{min} than S1 is obtained whereas for operating point 2 and operating pint 4 the same.

S3 Strategy. The last approach includes the optimization of the RMS value with varying amplitudes in different frequency bands. Four different sub-bands for each signal are chosen in order not to increase the number of decision variables too much and by doing so to limit the increase in the computation time.

In total for the current application there are 20 optimization variables, as there are four sub-bands for every operating point and four RMS values. The resulting values can be found in Table 4. Operating points 2 and 4 have been improved whereas for operating points 1 and 3 the amplitude optimization does not improve the result of the frequency optimization.

In S3 strategy the frequency region is divided in 4 subbands, which can either fully selected or not whereas in S2 strategy the frequency is a degree of freedom and can vary and thus improving the result (see Figure 2).

By studying the tables for the different strategies it can be seen that the frequency optimized strategy gives results in average of high quality in a reasonable computation time.

4.2 Comparison to White Noise Inputs

For consolidating the above results a comparison with white noise inputs has been carried out. The white noise has been chosen in order to have the same RMS value as the original signal and it is added to the operating points.

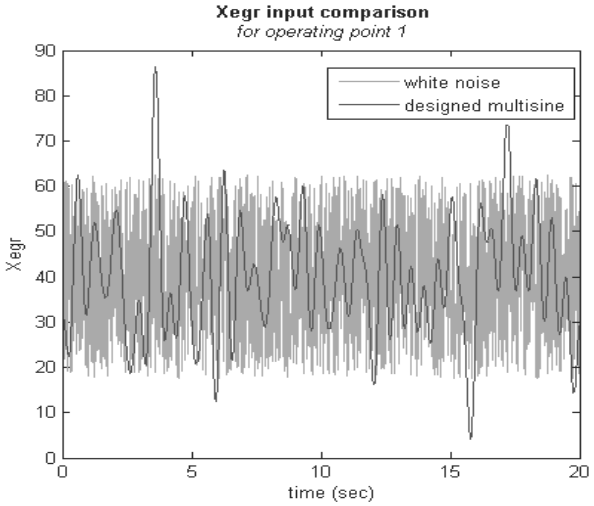

Figure 4. Comparison of X_{egr} input in multisine and white noise form.

		Frequency band values			
O.P.	λmin	X_{egr}	X_{vgt}	n	W_{f}
1.	1.39*e*04	[0.20-1.00]	[0.30-1.06]	[0.05-1.39]	[0.13-1.00]
2.	2.92*e*06	[0.05-2.00]	[0.05-5.00]	[0.05-2.00]	[0.05-4.00]
3.	7.34*e*03	[0.43-1.00]	[0.05-1.90]	0.05-1.58]	[0.14-1.00]
4.	1.99*e*07	[0.06-2.00]	[0.06-5.00]	[0.06-2.00]	[0.06-4.00]

Table 3. Frequency optimization results.

O.P.	λ_{min}	X_{egr}		X_{vgt}		n		W_{f}	
		RMS	A_k	RMS	A_k	RMS	A_k	RMS	A_k
1.	1.21*e*04	12.80	0.68/0.98/0.18/0.00	4.98	1.00/ 0.405/ 0.12/ 0.00	190.00	0.85/ 0.00/ 0.48/ 0.12	4.78	0.65/ 0.00/ 0.00/ 0.00
2.	3.38*e*06	12.7803	0.00/ 1.00/ 0.00/ 0.95	0.44	0.92/ 0.97/ 0.93/ 0.93	299.99	0.98/ 0.93/ 0.98/ 0.96	2.66	0.95/ 0.96/ 0.92/ 0.97
3.	2.84*e*03	12.19	0.97/ 0.99/ 0.98/ 0.80	8.00	1.008/ 0.99/ 0.98/ 0.10	270.00	0.98/ 0.99/ 0.95/ 0.96	1.99	0.97/ 0.99/ 0.96/ 0.96
4.	2.30*e*07	5.0967	0.50/ 0.50/ 0.50/ 0.50	8.00	0.50/ 0.50/ 0.50/ 0.50	194.34	0.50/ 0.50/ 0.50/ 0.50	1.50	0.50/ 0.50/ 0.50/ 0.50

Table 4. Results of RMS optimization with different amplitudes for different frequency bands.

Table 5 summarizes a complete comparison. The minimum eigenvalue for the white noise shown in the table is the mean value of ten different trials in order to ensure an adequate comparison. Figure 4 displays the X_{egr} input for the S1 and the white noise case. The λ_{min} of the white noise is between 200-600 whereas with the multisines 10^3 - 10^6 higher values are achieved.

	λ_{min}		
O.P.	RMS optimized	frequency optimized	white noise
1.	3.7855*e*03	1.3893*e*04	228.05
2.	2.9155*e*06	1.4303*e*04	366.23
3.	2.4572*e*03	7.3435*e*03	237.59
4.	1.9915*e*07	1.9915*e*07	662.76

Table 5. Comparison for optimization of the RMS, frequency and white noise.

4.3 Identification

The designed inputs are applied to a real engine. A production 2 liter EU5 common rail Diesel engine mounted on a dynamical engine test-bench was used in the current work. The generated outputs are used for identifying the model's parameters.

The designed inputs were applied on a real system, the measured outputs where used for PE. The resulting pa- rameters were used to simulate outputs. Figure 6 illus- trates the engine outputs (measurements) together with the simulated outputs from the designed inputs of the third operating point. The designed input is applied from 5 to 25 seconds. It can be seen that the calibrated model accurately describes the measurements. The resulting pa- rameters together with their confidence bounds can be found in Table 6. The confidence bounds indicate that the estimation is accurate. Which are typically at least the order of magnitude smaller than the parameter values.

4.4 Validation

In the above subsection parameters were obtained through identification for OP 4. In the current subsection designed inputs for OP 2 were applied to the real engine, while the simulator used the previously obtained parameters from OP 4 to predict the outputs.

The simulated outputs are following the engine outputs as seen in Figure 6. The SSE value for this estimation is SSE = 1.45e+03. This validation corroborates the proposed method.

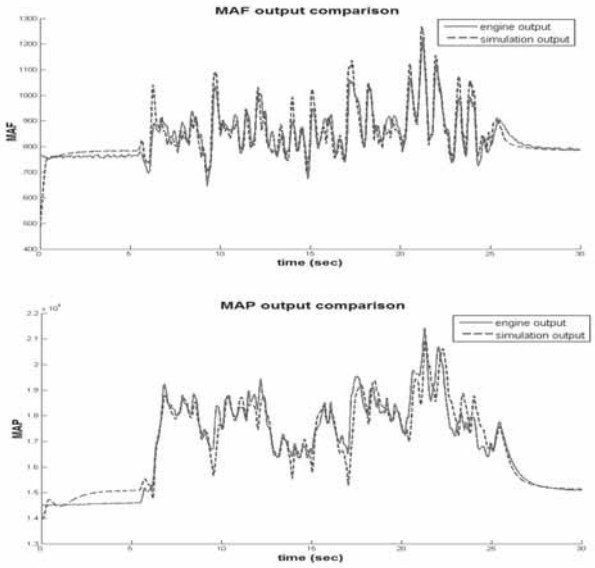

Figure 5. Output comparison.

5 Conclusion

In this work the dynamic parameters of an airpath model for a 2 liter EU5 common rail Diesel engine with external exhaust gas recirculation and a variable geometry turbine turbocharger have been accurately estimated. To ensure parameter accuracy, optimal random multisine inputs have been designed based on Optimal Experiment Design techniques.

Parameter Estimation with real engine measurements for operating point 4		
parameter	found value	95% conf.bound
V_i	0.0183	± 6.59e-04
V_x	0.0100	± 7.78e-04
η_n	0.7098	± 1.48e-03
τ_{egr}	0.2161	± 9.28e-03
τ_{vgt}	0.5620	± 9.56e-03
SSE	1.222e+03	
MSE	0.4078	

Table 6. Test-bench measurements results.

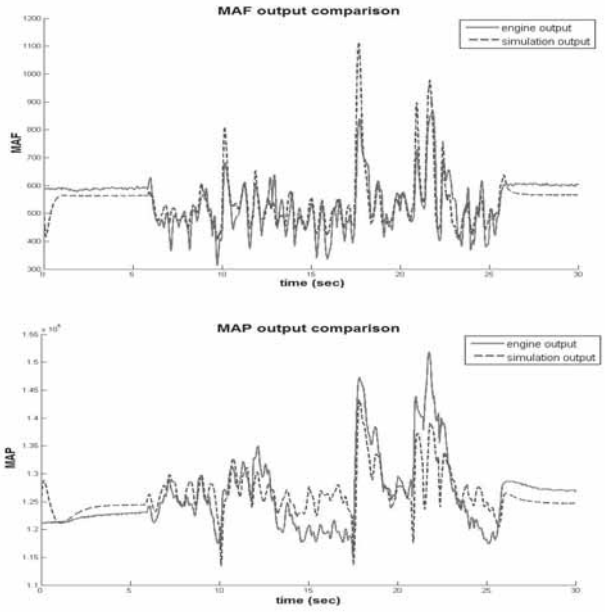

Figure 6. Output comparison validation.

Three input optimization profiles have been presented. The use of multisines allows exclusive excitation of a specific frequency band of interest. Moreover, fast dynamics are included without increasing the number of discretization variables. The results have provided an ac- ceptable prediction both in identification as in validation.

ACKNOWLEDGEMENTS

This research is upported by rojects OT/10/035, PFV/10/002 (Center-of-Excellence Optimization in Engineering) of the Research Council of the KULeuven, Project KP/09/005 (SCORES4CHEM) of the Industrial Research Council of the KULeuven, the Belgian Program on Interuniversity Poles of Attraction, initiated by the Belgian Federal Science Polic Office and the industry project ACCM. D.
Telen has a Ph.D grant of the Institute for the Promotion of Innovation through Science and Technology in Flanders (IWT- Vlaanderen). J. Van Impe holds the chair Safety Engineering sponsored by the Belgian chemistry and life sciences federation essenscia. The scientific responsibility is assumed by its authors.

REFERENCES

[1] Alberer, D. (2009). *Fast Oxygen Based Transient Diesel Engine Control*. Ph.D. thesis, J.K. Universität Linz.

[2] Balsa-Canto, E., Alonso, A., and Banga, J. (2010). An iterative identification procedure for dynamic modeling of biochemical networks. *BMC Systems Biology*, 4.

[3] Biegler, L. (2007). An overview of simultaneous strategies for dynamic optimization. *Chemical Engineering and Processing: Process Intensification*, 46, 1043–1053.

[4] Diehl, M., Bock, H., Schlöder, J., Findeisen, R., Nagy, Z., and Allgöwer, F. (2002). Real-time optimization and nonlinear model predictive control of processes governed by differential-algebraic equations. *Journal of Process Control*, 12, 577–585.

[5] Ferreau, H.J., Ortner, P., Langthaler, P., del Re, L., and Diehl, M. (2007). Predictive control of a real-world diesel engine using an extended online active set strategy. *Annual Reviews in Control*, 31(2), 293–301.

[6] Franceschini, G. and Macchietto, S. (2008). Model-based design of experiments for parameter precision: State of the art. *Chemical Engineering Science*, 63, 4846–4872.

[7] Ljung, L. (1999). *System Identification: Theory for the User*. Prentice Hall.

[8] Pintelon, R. and Schoukens, J. (2001). *System Identification, A Frequency Domain Approach*. IEEE Press.

[9] Puchner, S., Winkler-Ebner, B., Alberer, D., and del Re, L. (2009). Optimization based mean value model of turbocharged diesel engines. In *MATHMOD 2009 - 6th Vienna Int. Conference on Mathematical Modelling*.

[10] Stewart, G., Borrelli, F., Pekar, J., Germann, D., Pachner, D., and Kihas, D. (2011). *Automotive Model Predictive Control: Models, Methods and Applications*, chapter Towards a Systematic Design for Turbocharged Engine Control, 211. Springer.

[11] Walter, E. and Pronzato, L. (1997). *Identification of Parametric Models from Experimental Data*. Springer, Paris.

Submitted MATHMOD 2012: November 2011
Accepted MATHMOD 2012: January 2012
Submitted SNE Revised: October 2012
Accepted: December 5, 2012